Nonisothermal Single- and Two-Phase Flow Through Consolidated Sandstones

N. ARIHARA*
H. J. RAMEY, JR.
W. E. BRIGHAM
MEMBERS SPE-AIME

STANFORD U.
STANFORD, CALIF.

ABSTRACT

This study concerns nonisothermal single- and two-phase flow of a single-component fluid (water) in consolidated porous media. Linear flow experiments through cylindrical consolidated cores were performed. Both natural (Berea) and synthetic cement-consolidated sand cores were used. Fabrication of the synthetic sandstones was important to permit reproducible fabrication of high-porosity, low-permeability sandstones with thermowells, pressure ports, and glass-tube capacitance probe guides cast in place.

Both hot-fluid and cold-water injection experiments were carried out in natural and synthetic sandstones. The thermal efficiency of hot-water and cold-water injection was found to depend on heat injection rate: the higher the heat injection rate, the higher the thermal efficiency. One important result of this study is that much of the previous work with nonisothermal single-phase flow in unconsolidated sands may be extended to consolidated sandstones despite the differences in the isothermal flow characteristics of these systems.

In two-phase boiling flow experiments, hot, compressed liquid water entered the upstream end of the core, moved downstream, started vaporizing, and flowed through the remainder of the core as a mixture of steam and liquid water. Significant decreases in both temperature and pressure occurred within the two-phase region. Even for large temperature changes, it was found that two-phase flow can be nearly isenthalpic and steady state if heat transfer between the core and the surroundings is at a low level.

INTRODUCTION

Geothermal energy is being given much attention as a new source of energy. Prime questions in geothermal energy extraction are (1) how much energy can be recovered, and (2) how fast can it be extracted? To find useful answers to these questions, the basic nature of the boiling flow of water in porous media must be understood.

Literature on oil recovery by hot-fluid injection and underground combustion presents some of the important features of nonisothermal, two-phase flow that appear pertinent to geothermal reservoirs.

The injection of hot water to effect oil recovery was commonly considered before 1930. In 1930, Barb and Shelley[1] mentioned a rumor that hot-water flooding had been tried in New York State and abandoned because of excessive cost. The heating and economic results of hot-water injection were evaluated in this pioneering study.

The next study of heat transport in a formation caused by hot-fluid injection was presented by Stovall[2] in 1934. Both laboratory and field experiments were described. Field determination of both wellbore heat losses and vertical losses from a heated formation were described in this remarkable study. Apparently, the next study of vertical heat loss on hot-fluid injection was published by Lauwerier[3] in 1955. It was assumed that injection rate, V_w, and temperature, T_i, would remain constant; thermal conductivity in the direction of flow was zero; and the thermal conductivity in the flooded layer perpendicular to the direction of flow was infinite so that the temperature in the flooded layer, T_1, was always constant at a given location in the flooded zone. Prats[4] has called the latter condition the "Lauwerier assumption." The conductivity in the overburden and underburden, λ_2, was assumed to be finite and constant. The loss of of heat from the injected fluid to the adjacent strata resulted in a decrease in temperature in the direction of flow. Lauwerier derived the temperature both in the injection interval and the adjacent strata as a function of time and distance.

In 1959, Marx and Langenheim[5,6] presented a solution for a heat-loss problem related to the one considered by Lauwerier, but where the heated region remained at a constant temperature equal to the injection temperature. Vertical heat loss reduced the size of the heated region.

Rubinstein[7] introduced the concept of the fraction of cumulative heat injected loss to adjacent strata,

Original manuscript received in Society of Petroleum Engineers office March 13, 1975. Paper accepted for publication July 16, 1975. Revised manuscript received March 8, 1976. Paper (SPE 5380) was first presented at the SPE-AIME 45th Annual California Regional Meeting, held in Ventura, April 2-4, 1975.

*Now with Arabian Oil Co., Tokyo, Japan.

[1]References given at end of paper.

This paper will be included in the 1976 *Transactions* volume.

W_o^*, and presented the heat loss for a radial flow model of hot-water injection with fewer assumptions than used by Lauwerier. The utility of the W_o^* concept was extended by calculation of the cumulative heat loss for the Marx-Langenheim and and Lauwerier solutions.[8]

Spillette[9] solved the energy-balance equation numerically with the same assumptions as Rubinstein. The primary effects of including horizontal heat conduction in the analysis are the lowering of the calculated sand temperatures near the injection front and the propagation of injected energy further into the reservoir.

Baker[10-12] conducted a series of experimental studies of heat transfer in hot-fluid injection with a radial flow model and observed that thermal efficiencies, $E = 1 - W_o^*$, increased with increasing rates of heat injection. His unique experimental work led to the work of Ersoy[13] and Crichlow.[14]

Crichlow[14] also found flow-rate sensitivity of thermal efficiency in hot-fluid injection experiments, although results for steam injection were not consistent. He explained thermal-efficiency dependence on injection rate by the presence of a film coefficient at the boundary between the core and the core-holder tube.

Although much work has been done in the study of oil recovery by steam injection, there has been no specific study of nonisothermal boiling, two-phase flow of water through porous media. However, in 1951, Miller[15] presented experimental results and analysis of single-component boiling, two-phase flow of propane.

There also has been a significant amoun of work presented on the simulation of thermal oil recovery processes that involve steam injection. Among them, the works of Coats *et al.*[16] and Weinstein *et al.*[17] are comprehensive.

Although work on thermal recovery of oil has been based on sound laboratory experimentation for specific oil recovery processes, there appears to have been only limited experimental work aimed directly at geothermal fluid systems. See Cady *et al.*,[18] and note the bibliography. However, the work of Cady *et al.* involved batch production of water and steam from a hot porous medium.

The main purpose of the study reported herein was development and operation of apparatus suitable for *both* continuous and batch geothermal fluid flow experiments. The experimental data were intended to permit study of phenomena important to geothermal systems, and to permit comparisons between the experimental results and mathematical simulations. This paper presents the first phase of the study—development of the apparatus and experimental results for a variety of experiments pertinent to production and reinjection of geothermal fluids.

EXPERIMENTAL EQUIPMENT

A bench-scale model was designed to permit an examination of thermodynamic and fluid-mechanic aspects of two-phase boiling flow. A variety of important peripheral experiments were conducted with the same apparatus. For example, cold-water injection into a system initially containing hot water is an important operation for geothermal heat scavenging from the rock matrix by cold-condensate injection.

A schematic diagram of the completed apparatus is shown in Fig. 1. Cold feedwater is pumped through a tubular furnace and into a core contained in a Hassler-sleeve core holder. The core holder is placed within an air bath used to set ambient temperatures as high as 410 °F. An accumulator is located immediately downstream of the pump to reduce flow pulsations.

Flow rate is measured both upstream by a flowrator and downstream of the core by timed weighing of the efflux. Both regulating and metering valves are used to adjust the backpressure and flow rate. Helicoid pressure gauges are installed on each side of the core. Porous metal filters (60-micron elements) are located before the tubular furnace and before the backpressure valve.

The temperature of the flowing fluid is measured after the tubular furnace, at the core inlet and exit, and throughout the entire length of the core by way of a traversing thermocouple. The traversing thermocouple is a 1/25-in.-diameter sheathed thermocouple inside 1/16-in.-OD stainless steel tubing. Pressures are measured at the inlet and outlet of the core, and at three locations along the core by means of pressure transducers.

A detailed description of the major equipment components follows.

CORE HOLDER

A modification of a Hassler-type core holder designed by the Marathon Oil Co. was used. Fig. 2 shows a detailed drawing of the core holder. It consists of an outer shell, the Viton tubing, and end pieces. The shell is 26 in. long × 3.5 in. OD, with a 0.438-in. wall thickness. The shell has four entry ports or taps, one for the overburden pressure and three for pressure measurements at 6-in. intervals along the core. More pressure taps may be used. The Viton tubing is 26 in. long × 2.5 in. OD, with a 0.25-in. wall thickness. The inlet plug has taps for inlet flow and pressure measurement. The outlet plug has taps for exit flow, a pressure tap, and a hole through which the guide tubing for the saturation probe passes. A thermocouple well for the traversing thermocouple passes through the tap for exit flow and through a heat-exchanger-type fitting. The materials used in the core holder are 304 stainless steel for the outer shell and the compression ring, and brass for the other parts. The core holder and end plugs are secured by end plates and four tie rods.

POROUS MEDIA

Two types of porous media were used: a Berea sandstone core and several synthetic consolidated sandstone cores. In the case of the Berea core, a groove was cut on the side surface and 1/16-in.-OD

stainless steel tubing with one end plugged by silver solder was cemented in the groove.

Fondu calcium aluminate cement, silica sand of about 100 Tyler mesh size, and water were used to make the synthetic cores. The proportions were 80-percent sand and 20-percent cement, by weight. The sand-cement mixture was prepared by thoroughly mixing sand with the blending water (0.5 percent by weight) and then with cement. The mixture was poured into a mold formed with plastic tubing in which glass tubing for the liquid saturation probe and a thermocouple tube were held in place. While pouring the sand, the mold was tapped and vibrated to compact the sand. Water was injected until breakthrough, and the mold was then allowed to hydrate for 1 day. After 24 hours, the plastic tubing was peeled off and the core was shaped to a desired size: 2 in. OD × 23.5 in. long. This method of making artificial sandstone cores was found to be reproducible. For the mixture of 80-percent sand and 20-percent cement, the permeability and porosity were about 100 md and 35 percent of bulk volume, respectively. This combination of low permeability and high porosity was ideal for the purposes of this study.

SATURATION PROBE

Although not described in this paper, one objective of this study was detection of the liquid content in the porous media to aid in preparation of relative permeability information. It has been mentioned that a liquid-saturation (content) probe guide was cast in the artificial porous media. The liquid-content probe was described by Baker. This

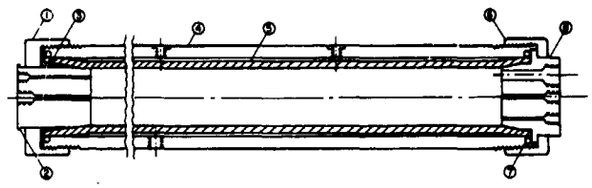

FIG. 2 — CORE HOLDER, (1) CAP, BRASS; (2) INLET PLUG, BRASS; (3) COMPRESSION RING, 304 STAINLESS STEEL; (4) SHELL, 304 STAINLESS STEEL; (5) SLEEVE, VITON; (6) CAP, BRASS; (7) O-RING 2-233, VITON; (8) OUTLET PLUG, BRASS.

device appeared most readily adaptable to detection of liquid contents at geothermal-system temperatures. Details of the Baker probe may be found in Ref. 19. It is not the purpose of this paper to describe this device further.

PRESSURE MEASUREMENT

The inlet and outlet pressures and the pressure differences across the intervals along the core were measured with differential pressure transducers. To gain pressure data at intervals along the core, taps were made through the sidewall of the shell and the Viton-sleeve tubing. A flanged penetrator with O-rings provided pressure-tight passage through the sleeve.

EXPERIMENTAL PROCEDURE

Single-phase experiments were performed first. Absolute permeability to gas and water was measured over a range of temperatures. The injected fluid was heated by the tubular furnace to the constant temperature of the core.

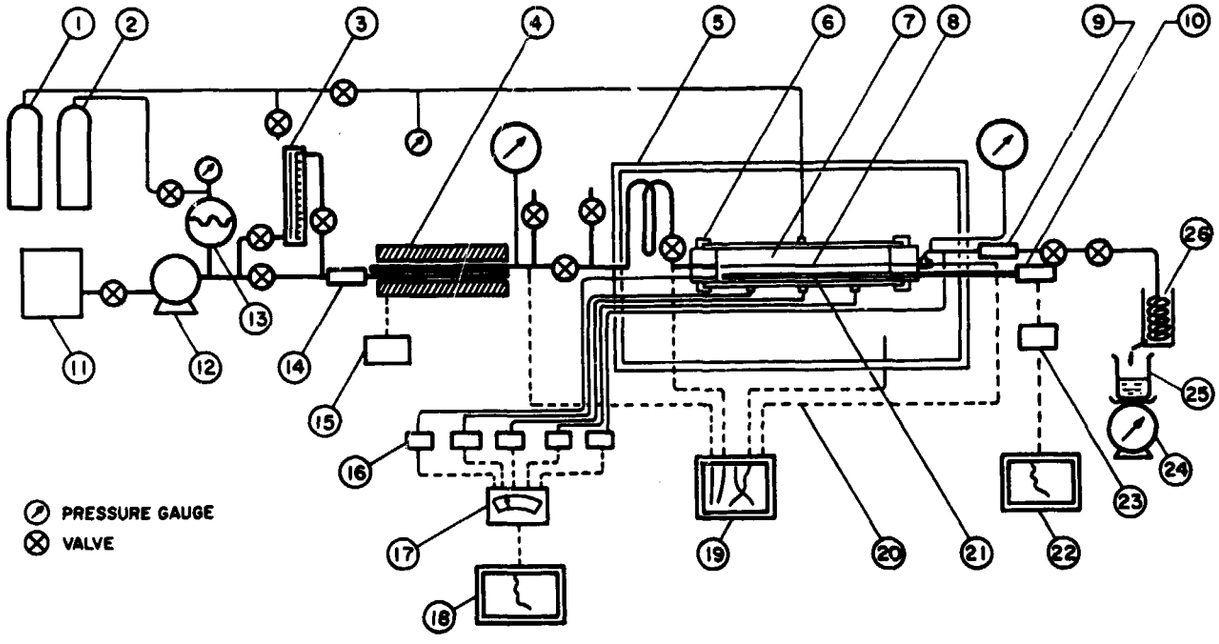

FIG. 1 — SCHEMATIC DIAGRAM OF APPARATUS. (1) N_2; (2) N_2; (3) FLOWRATOR; (4) TUBULAR FURNACE; (5) OVEN, INSIDE DIMENSIONS 41¼ × 17½ × 24 IN.; (6) CORE HOLDER; (7) CORE; (8) TRAVERSING THERMOCOUPLE; (9) FILTER; (10) FILTER; (11) WATER FEED; (12) PUMP; (13) ACCUMULATOR; (14) FILTER; (15) TEMPERATURE CONTROLLER; (16) PRESSURE TRANSDUCER; (17) PRESSURE INDICATOR; (18) RECORDER; (19) RECORDER; (20) THERMOCOUPLES; (21) SATURATION PROBE; (22) RECORDER; (23) AC-DC CONVERTER; (24) BALANCE; (25) COLLECTOR; (26) HEAT EXCHANGER.

The procedure used in making a run was similar for injection of either hot water or steam. The pump and the tubular furnace were turned on and set for certain pressure and temperature levels, and the hot fluid was vented until the temperature of the injected fluid reached the desired level. Then the bypass valve was closed and the inlet pressure was set by the relief valve in the pump. The flow rate, or outlet pressure was regulated by adjusting the outlet valves. The temperature of injected fluid and the pressure drop across the whole length of the core were recorded continuously. The flow rate was measured periodically. Temperatures along the core were measured by traversing the thermocouple. The sensing time per point was 6 seconds, although a value as low as 1.5 seconds could have been used.

The procedure for the cold-water injection experiments was the same as for the hot-fluid injection, except that the core was initially heated and set to maintain a constant temperature instead of heating the injected fluid.

The main experiment considered under the category of two-phase flow experiments was the steady injection of hot, compressed liquid water into the core at a rate such that a boiling front would form somewhere within the core length, leading to an obvious two-phase flow region with declining temperature and pressure. Pressure declined because of boiling two-phase flow, and temperature declined to maintain the vapor pressure-temperature relationship for water. The experimental procedure was as follows.

First, the core was saturated with water and heated to an initial temperature and pressure well within the compressed liquid region. During the heating procedure, hot water was circulated at a low rate through the core, with the outlet conditions maintained in the liquid region. After temperatures along the axis of the core stabilized, two-phase flow was initiated by opening the outlet valve and increasing the pressure drop across the core. A variety of experimental conditions could be obtained by changing the inlet temperature and the pressure drop across the core. Pressures at the five transducer taps, and temperature, were measured in the axial direction. It was possible to achieve approximate steady-state temperature and pressure distributions.

RESULTS

ISOTHERMAL SINGLE-PHASE FLOW

The permeability of a porous medium to a single-phase gas usually exceeds the permeability of the same porous medium to a single-phase liquid. The difference in these permeabilities is caused by the phenomenon known as slip and by reactions between liquids and the solid. The first studies concerned an investigation of the effect of temperature level on the absolute permeability to both gas and water for the synthetic cores. No such information had been presented previously to our knowledge.

Klinkenberg[20] developed the relation between the permeability of a porous medium to gas and to a nonreactive liquid:

$$k_a = k\left(1 + \frac{4C}{r}\,\frac{RT}{\sqrt{2\pi}p_m N d^2}\right) = k\left(1 + \frac{b}{p_m}\right), \quad \ldots\ldots\ldots (1)$$

where k_a is the apparent or observed permeability to gas and k is the absolute permeability to gas at high pressures (equal to the absolute permeability to a single-liquid phase for nonreactive solids). (Other symbols are defined in the Nomenclature.) The constant, b, is often referred to as the Klinkenberg factor, which is constant for a given gas and a given porous medium at a constant temperature. From Eq. 1, the Klinkenberg factor should be directly proportional to temperature.

Fig. 3 presents the measured permeabilities to nitrogen for a synthetic sandstone core plotted vs the reciprocal mean core pressure for a variety of temperatures ranging from 75 to 342 °F. All data can be represented by a single line, indicating no significant effect of temperature level for the range of temperatures studied, although the slope of the line, kb, should change in proportion to temperature according to Eq. 1. A possible explanation is that the proportionality factor, C, may be inversely proportional to temperature for this case. The Klinkenberg factor is 3.77 psi, much higher than would be expected from correlations for natural sandstone cores. Also shown on the ordinate of Fig. 3 is the absolute permeability to water for the same synthetic core, 98 md (76 to 340 °F). This is a few percent lower than the extrapolated absolute permeability to gas, 100 md.

Although not evident in Fig. 3, the same permeability to water was measured for a range of temperatures from 76 to 340 °F. Similar results were found for Berea sandstone for a temperature range from 70 to 320 °F. This was unlike previous findings by Weinbrandt *et al.*,[21] wherein a strong temperature effect was found for water flow. One significant difference was that the confining pressure was only

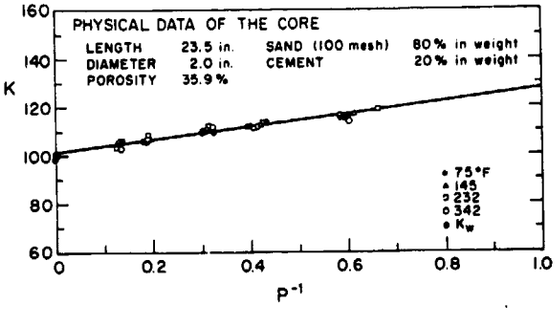

FIG. 3 — PERMEABILITY TO NITROGEN VS RECIPROCAL MEAN PRESSURE FOR A SYNTHETIC SANDSTONE CORE.

400 psi for the present studies, as compared with several thousand psi for the Weinbrandt *et al.* study. This compound effect of the confining pressure and temperature on the permeability to liquid was investigated by Cassé[22] recently. According to his results, temperature has only a minor effect on the absolute permeability to water at low confining pressure. This is consistent with the findings of this study.

NONISOTHERMAL SINGLE-PHASE FLOW

A series of hot-water injection experiments was made for each core at varying injection rates and injection temperatures. In these experiments, hot water was injected into a core initially containing cold water. Fig. 4 presents temperature vs distance along the core for a typical run. From these data, it is possible to compute the effective thermal conductivity in the direction of flow and the heat loss radially from the core. As can be seen in Fig. 4, heat flow changes from an unsteady state at early stages to a nearly steady-state process at long times. The temperature distribution along the core shows transient heating curves for short times. At long times, the incremental changes in point temperatures become smaller, and eventually the temperature profile stabilizes. The temperature is nearly linear along the axis of the core. At steady-state conditions, the *net* heat injection rate is exactly balanced by the radial heat loss from the system.

To evaluate the experimental results, a mathematical model similar to the one of Lauwerier[3] can be used. In the present work, the core is cylindrical and the heat transfer from the core to the surroundings can be expressed by forced convection, rather than conduction. In addition to these differences from Lauwerier's model, the injection temperature is a continuous function of time rather than a constant.

Applying a heat balance to the hatched region of Fig. 5, the following equation may be written:

$$r_o \rho_o C_1 \frac{\partial T}{\partial t} + r_o \rho_w V_w C_w \frac{\partial T}{\partial x} + 2UT = 0 \ , \quad \ldots (2)$$

where

$$T = T_1 - T_\infty$$

and

$$\rho_1 C_1 = (1 - \phi)\,\rho_S C_S + \phi \rho_w C_w \quad \ldots (3)$$

Derivation of Eq. 2 requires the Lauwerier assumption (see Prats[2]) that temperature within the injection interval is constant in a vertical plane. This is equivalent to the assumption of an infinite thermal conductivity in the radial direction. It is also assumed that convective heat transport within the interval is much greater than the conductive heat transport (see Crichlow[14]) or that the thermal conductivity in the axial direction is zero.

Introducing the dimensionless variables ξ and τ defined by,

$$x = \frac{r_o \rho_w V_w C_w}{2U}\,\xi, \quad t = \frac{r_o \rho_1 C_1}{2U}\,\tau, \quad \ldots (4)$$

the problem to be solved now can be expressed as

$$\frac{\partial T}{\partial \tau} + \frac{\partial T}{\partial \xi} + T = 0, \text{ for } \xi > 0, \ \tau > 0 \ , \quad \ldots (5)$$

$$T = T_1 - T_\infty = F(a\tau),$$

$$\text{for } \xi = 0, \ \tau > 0 \quad \ldots (6)$$

$$T = 0, \text{ for } \xi > 0, \ \tau = 0 \quad \ldots (7)$$

and

$$a = \frac{r_o \rho_1 C_1}{2U} \ . \quad (a\tau = t) \quad \ldots (8)$$

The condition given by Eq. 6 permits the injection temperature to be an arbitrary function of time. This was necessary because the heat capacity of the apparatus inlet required that the injection temperature increase during heat injection experiments. Thus, a variable injection temperature in the analytical solution permitted matching experimental conditions reasonably well.

The solution can be obtained by using the Laplace transformation, yielding

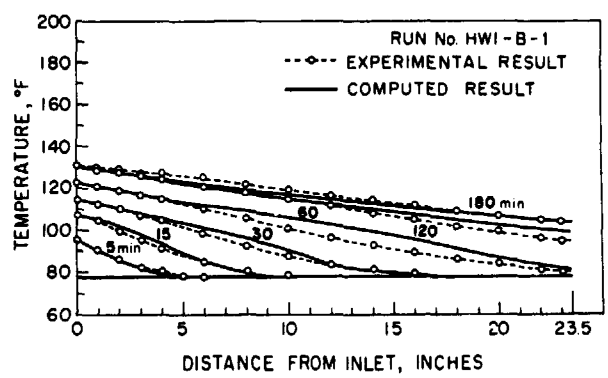

FIG. 4 — COMPARISON OF CALCULATED WITH EXPERIMENTAL TEMPERATURE DISTRIBUTIONS FOR HOT-WATER INJECTION, BEREA SANDSTONE. (INJECTION RATE = 14.0 GM/MIN, INJECTION PRESSURE = 250 PSIG, PRESSURE DROP = 22 TO 13 PSI. SEE REF. 19 FOR COMPLETE DATA.)

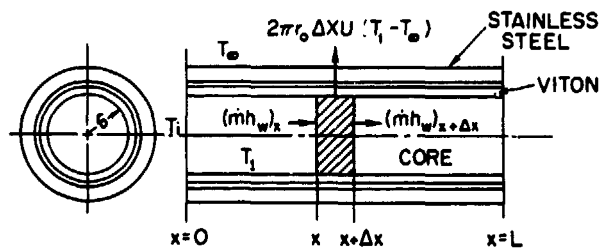

FIG. 5 — HEAT BALANCE ON CORE ELEMENT.

$$T_1 = T_\infty + e^{-\xi} F(a\tau - a\xi)\ \alpha\ (\tau - \xi)\ , \quad \ldots\ldots\ldots\ldots\ldots\ldots\ldots\ldots (9)$$

or

$$T_1 = T_\infty + \exp\left(\frac{2UX}{r_o\rho_w V_w C_w}\right) F\left(t - \frac{\rho_1 C_1 X}{\rho_w C_w V_w}\right) \cdot \alpha\left(\frac{2U}{r_o\rho_1 C_1}\, t - \frac{2UX}{r_o\rho_w V_w C_w}\right) , \quad \ldots (10)$$

where

$$\alpha(\tau - \xi) = 1 \text{ for } \tau \geq \xi$$

$$0 \text{ for } \tau < \xi\ . \quad \ldots (11)$$

As shown in the experimental results, $F(t)$ is a function of time that can be expressed as $F(t) = T_\infty(1 - e^{-\beta t})$, where T_∞ and β are constants.

Fig. 4 shows an example of the calculated temperature distributions at various times. Fig. 6 presents the temperature of the core at the inlet end, $[F(t) + T_\infty]$, vs injection time. For the calculation, the following constants were used:

ρ_S = 165.4 lb/cu ft
C_S = 0.21 Btu/lb-°F
ρ_w = 62.0 lb/cu ft
C_w = 1.0 Btu/lb-°F
ϕ = 22 percent
U = 1.246 Btu/hr-sq ft-°F .

The values of ρ_S, C_S, ρ_w, and C_w given above are for the average temperature. U was calculated from the experimental data at steady state, as shown in Ref. 19.

The observed and calculated temperature distributions of Fig. 4 show some differences. The prime reason is that the over-all heat-transfer coefficient was assumed to be constant throughout the run. Actually, the over-all coefficient, U, has a higher value early in the heating process.

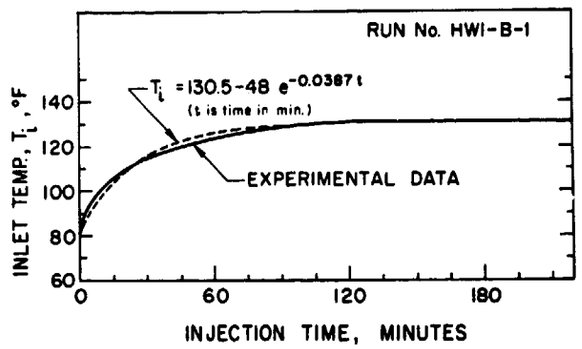

FIG. 6—TEMPERATURE HISTORY AT THE INLET OF THE CORE BEREA SANDSTONE.

With regard to radial heat loss, two important factors can be determined: (1) the thermal efficiency of the hot fluid injection, and (2) the over-all heat-transfer coefficient between the core within the sleeve and the surroundings.

Using the temperature distributions as shown in Fig. 4, thermal efficiencies were computed by numerical integration. Thermal efficiency is defined as the ratio of the heat within the injection interval to the cumulative heat injected at any time. Or,

$$E = \frac{H_s}{H_i}\ , \quad \ldots\ldots\ldots\ldots\ldots\ldots (12)$$

where the heat within the interval, H_s, is

$$H_s = \int_V \rho_1 C_1 (T_1 - T_o)\ dV\ , \quad \ldots (13)$$

and the cumulative heat injected is

$$H_i = \int_0^t q\rho_w C_w\ (T_i - T_o)\ dt\ \ldots (14)$$

Fig. 7 shows the result for the Berea sandstone core. Thermal efficiency is plotted vs cumulative heat injected, with heat injection rate as a parameter. Clearly, thermal efficiency depends on heat injection rate. The greater the rate of heat injection, $\dot{m}C_w\Delta T$, the higher the thermal efficiency. This trend was first observed by Baker,[10] and was verified by Ersoy[13] and Crichlow.[14]

Dependency of thermal efficiency on flow rate was not indicated by any of the early analytical studies.[3,5,7] It appears that Crichlow's[14] conclusion that the over-all heat-transfer coefficient is responsible is correct. That is, the higher the mass rate is, the higher will be the film coefficient between the fluid in the core and the core holder. Although this effect could also exist in field operations, the work of Crichlow[14] indicates that field velocities would be so low that the effect would not be significant. We now turn to cold water displacing hot water.

Because cold-water injection is the reverse

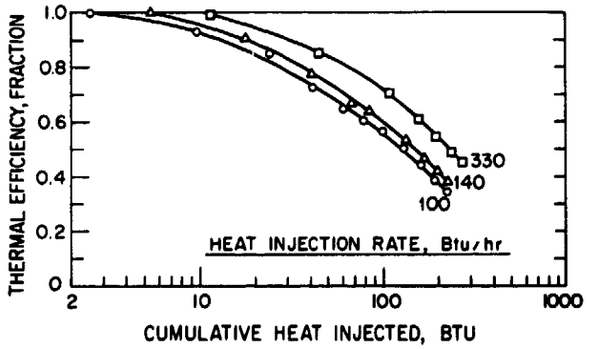

FIG. 7 — THERMAL EFFICIENCY AS A FUNCTION OF CUMULATIVE HEAT INJECTED IN HOT-WATER INJECTION, BEREA SANDSTONE.

procedure to hot-water injection, the same type of analysis can be performed. Fig. 8 presents the calculated and measured temperatures for various times. A reasonable agreement between computed and measured results is apparent from Fig. 8.

For this computation, the over-all heat-transfer coefficient measured for steady state was used for all injection times. This caused the calculated temperature distributions to be too low before the radial heat loss became steady state.

The constants used for the calculation of Fig. 8 were the same as those for Fig. 4, except the over-all coefficient, U, was changed from 1.246 to 2.384 Btu/hr-sq ft-°F. The cooling over-all coefficient, U, was almost twice that for heating runs. The difference between the values for the over-all coefficient on heating and cooling runs is surprising at first glance because the same apparatus was used in both cases. There was an important difference in procedure, however. During cooling runs, the core was heated to initial conditions by the air bath heaters with a hot-air circulating fan. During the heating runs, the initial condition was a core at room temperature without air circulation. Forced air circulation during the cooling runs increased the film coefficient outside the core holder and, consequently, increased the over-all coefficient.

The high over-all coefficient on cooling runs led to an apparent reversal in the dependency of thermal efficiency on heat injection rate (see Fig. 9). The core is cooled more efficiently when the heat injection rate, $\dot{m}C_w\Delta T$, is lower. Thus, for a specified injection period, higher values of heat injection rate result in more effective heat extraction from the surroundings. When water is injected with a constant-mass rate, the lower the injection temperature is, and heat is extracted more effectively from the surroundings within a certain period of time.

Some observations concerning pressure drop during cold- and hot-water flooding have been made. Weinstein *et al.*[17] applied a numerical model to cold-water flooding of a warm reservoir. Their study showed that (1) cold-water injection quickly cools the reservoir in the region surrounding the wellbore and accounts for most of the pressure drop across the reservoir; and (2) heating the injected water has a marked effect in decreasing the pressure drop. This also has been observed in the present study and can be explained through examination of Darcy's law. At constant-mass rate, the pressure drop across a certain length, ΔL, is proportional to μ_w/ρ_w. Both viscosity and density decrease as temperature increases, but viscosity drops far more rapidly. As a result, the pressure drop at 70 °F is about five times as large as at 300 °F.

TWO-PHASE FLOW EXPERIMENTS

A variety of two-phase boiling flow experiments were possible. Either cold or hot liquid could be injected into a hot core to cause hot liquid to boil by virtue of the pressure drop.

Fig. 10 presents temperature vs distance along the synthetic core for injection of cold water into a core initially containing hot water. The temperature surrounding the core was maintained at 385 °F. As can be seen in Fig. 10, cold water is heated by the core on flowing through it, then starts boiling at about 16 in. from the inlet. Once the liquid starts to boil, the temperature distribution in the two-phase flow region does not change with time.

Figs. 11 and 12 show temperature and pressure vs distance along the synthetic core at steady state

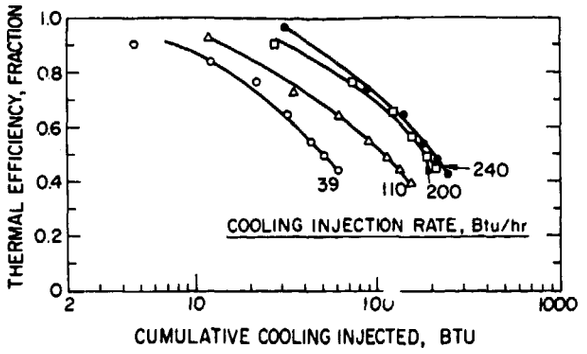

FIG. 9—THERMAL EFFICIENCY AS A FUNCTION OF CUMULATIVE COOLING INJECTED, BEREA SANDSTONE.

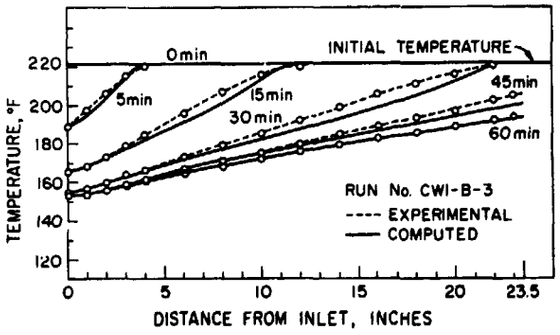

FIG. 8 — CALCULATED AND EXPERIMENTAL TEMPERATURES FOR COLD-WATER INJECTION, BEREA SANDSTONE. (INJECTION RATE = 24.2 GM/MIN, INJECTION PRESSURE = 247 PSIG, PRESSURE DROP = 13 TO 15.5 PSIG. (SEE REF. 19 FOR COMPLETE DATA.)

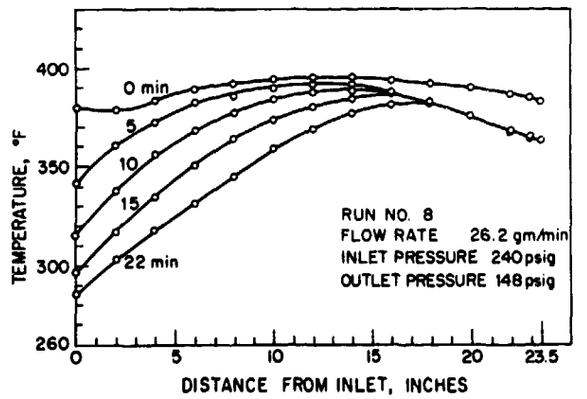

FIG. 10 — TEMPERATURE VS DISTANCE FOR TWO-PHASE FLOW, SYNTHETIC SANDSTONE. RUN 8 FLOW RATE, 26.2 GM/MIN.

for a range of flow rates and inlet conditions. Similar information for other runs may be found in Ref. 19. These figures show that it is experimentally possible to produce significant changes in both temperature and pressure within the two-phase boiling flow region. In these runs, the temperature of the injected water was nearly the same as the ambient temperature. Therefore, before developing two-phase flow by increasing the pressure drop across the core, single-phase (liquid) flow was isothermal. The transient period from single-phase to two-phase flow occurred very rapidly; then, the two-phase flow developed essentially a steady-state phase. The experimental results shown in Figs. 11 and 12 are useful for studying the thermodynamic and fluid mechanic behavior of two-phase boiling flow. Referring to Luikov,[23] mass and heat transfer in two-phase flow can be described by the following differential equations by assuming that flow is steady state and that ambient temperature, T_∞, is equal to the temperature of the water injected.

$$\frac{d}{dx}\left[\left(\frac{\rho_g k_g}{\mu_g}+\frac{\rho_\ell k_\ell}{\mu_\ell}\right)\frac{dp}{dx}\right]=0 \quad . \qquad (15)$$

$$\frac{d}{dx}\left(\lambda\frac{dT}{dx}\right)-h_{fg}\frac{d}{dx}\left(\rho_\ell\frac{k_\ell}{\mu_\ell}\frac{dp}{dx}\right)$$

$$+\left[\left(c_g\rho_g\frac{k_g}{\mu_g}+c_\ell\rho_\ell\frac{k_\ell}{\mu_\ell}\right)\frac{dp}{dx}\right]\frac{dT}{dx}$$

$$+\frac{p}{A}U\,(T_\infty-T)=0 \qquad (16)$$

where $T = T_s(p)$ is saturation temperature and a single-valued function of the pressure. Eq. 15 states that the total-mass rate is conserved. In Eq. 16, the first term is the gradient of conductive heat flux in the direction of flow; the second term is the gradient of latent heat for vaporization of water; the third term is the gradient of convective heat transfer; and the last term is the heat gain in the radial direction. Because all the terms but the first are positive in value, Eq. 16 indicates that in the direction of flow, the convective heat in the flowing fluid and the radial heat gain are balanced by conductive heat flux and latent heat of vaporization. To evaluate the effect of heat transfer by conduction in the flow direction and of convection from the surroundings, the first and fourth terms in Eq. 16 were calculated for the case of Run 4 in Ref. 19. The net heat flux coming into the core by conduction and convection can be obtained by computing

$$q(x)=\int_0^x\left[\frac{d}{dx}\left(\lambda\frac{dT}{dx}\right)+\frac{p}{A}U\,(T_\infty-T)\right]dx \quad . \quad . \quad . \qquad (17)$$

The results were plotted vs distance along the length of the core in Fig. 13. The heat flux carried by the flowing fluids (liquid and steam), calculated with the assumption of adiabatic conditions and no conduction, were also plotted in Fig. 13. Fig. 13 shows that the heat flux caused by conduction and radial convection are minor. From this result, it can be deduced that the flow is nearly isenthalpic. This means that the total enthalpy of the fluid is nearly constant at every section, although heat flow in the liquid and steam phases changes exponentially, as seen in Fig. 13.

CONCLUSIONS

1. As observed by Baker[12] and Crichlow,[14] the

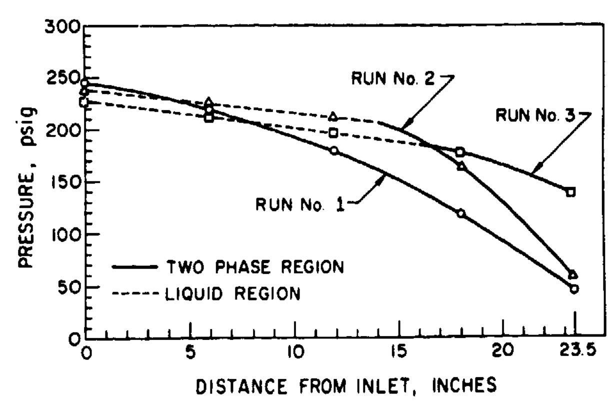

FIG. 12 — PRESSURE VS DISTANCE FOR TWO-PHASE STEADY FLOW, SYNTHETIC SANDSTONE.

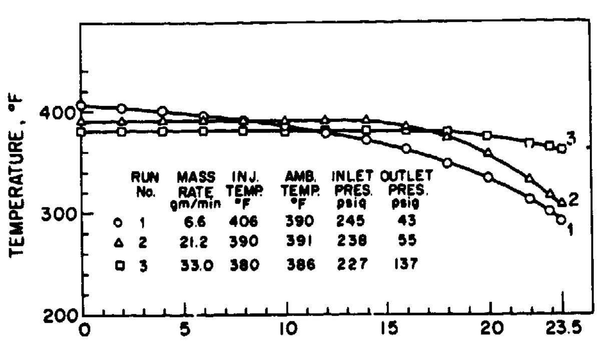

FIG. 11 — TEMPERATURE VS DISTANCE FOR TWO-PHASE STEADY FLOW, SYNTHETIC SANDSTONE.

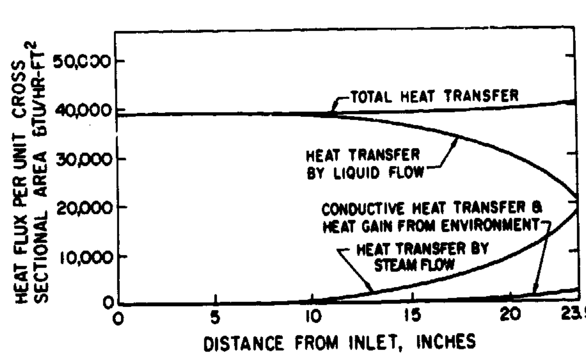

FIG. 13 — HEAT FLUX VS DISTANCE.

thermal efficiency of hot-water injection increases with increasing rate of heat injection.

2. The thermal efficiency for cold-water injection into a system initially containing hot water is injection-rate sensitive. The flow-rate sensitivity appears to be important under laboratory conditions only.

3. The dependence of thermal efficiency on heat injection rate is amplified if the over-all heat-transfer coefficient of the core holder increases. This appears to verify the Crichlow[14] observation that dependence of thermal efficiency on heat-injection rate is a film coefficient effect that is not likely to be important in field operations.

4. It is experimentally possible to develop in-place, boiling, two-phase flow with wide ranges of temperature and pressure drops and total-mass flow rate.

5. In-place boiling flow can be nearly steady state even when heat transfer exists in the direction perpendicular to flow.

NOMENCLATURE

a = constant, see Eq. 8
b = constant, see Eq. 1
C = proportionality constant
C_g = specific heat of gas
C_ℓ = specific heat of liquid
C_S = specific heat of solid rock
C_w = specific heat of water
C_1 = specific heat of core and contained fluids
d = collision diameter
E = thermal efficiency, fraction
h_{fg} = latent heat of vaporization
H_i = cumulative heat injected
H_s = cumulative heat in the injection interval
k = absolute permeability to gas
k_a = apparent permeability to gas
k_g = effective permeability to gas
k_ℓ = effective permeability to liquid
$\dot{m}$ = mass rate
N = Avogadro's number
p_m = mean pressure
q = volumetric injection rate, net heat flux
r = capillary radius
r_o = radius of the core, ft
R = universal gas-law constant
t = time
T = absolute temperature
T_s = saturation temperature (on vapor-pressure curve)
T_∞ = the ambient temperature, °F
U = the over-all heat-transfer coefficient, Btu/hr-sq ft-°F, based on the radius of the core
V = volume
V_w = flow velocity
x = distance in direction of flow
α = step function, see Eq. 11
λ = thermal conductivity
μ_g = viscosity of gas
μ_ℓ = viscosity of liquid
μ_w = viscosity of water
ξ = dimensionless group, see Eq. 4
ρ_g = density of gas
ρ_ℓ = density of liquid
ρ_S = density of solid rock
ρ_w = density of water
ρ_1 = density of core and contained fluids
τ = dimensionless group, see Eq. 4
ϕ = fractional porosity

ACKNOWLEDGMENTS

This research was carried out under Research Grant GI-34925 from the National Science Foundation. Financial aid from the National Science Foundation is hereby gratefully acknowledged. Helpful discussions have been held with many persons too numerous to list. Particularly noteworthy are S. C. Jones of Marathon Oil Co., who designed the core holder, and Paul E. Baker of Chevron Research Corp. Portions of this work were conducted by N. Arihara[19] to meet doctoral requirements at Stanford U.

REFERENCES

1. Barb, C. F. and Shelley, P. G.: "Production Data on Appalachian Oil Fields," Bull. No. 6, School of Mineral Industries, Pennsylvania State College (1930).
2. Stovall, S. L.: "Recovery of Oil From Depleted Sands by Means of Dry Steam," *Oil Weekly* (Aug. 13, 1934) Vol. 74, No. 9, 17.
3. Lauwerier, H. A.: "The Transport of Heat in an Oil Layer Caused by the Injection of Hot Fluid," *Appl. Sci. Res.* (1955) Vol. 5, Sec. A, 145.
4. Prats, M.: "The Heat Efficiency of Thermal Recovery Processes," *J. Pet. Tech.* (March 1969) 323-332; *Trans.*, AIME, Vol. 246.
5. Marx, J. W. and Langenheim, R. H.: "Reservoir Heating by Hot Fluid Injection," *Trans.*, AIME (1959) Vol. 216, 312-315.
6. Ramey, H. J., Jr.: "Discussion on Reservoir Heating by Hot Fluid Injection," *Trans.*, AIME (1959) Vol. 216, 364-365.
7. Rubinstein,* L. I.: "The Total Heat Losses in Injection of a Hot Fluid Into a Stratum," *Neft I Gaz* (1959) Vol. 2, No. 9, 41 (*sometimes spelled Rubinshtein).
8. Ramey, H. J., Jr.: "How to Calculate Heat Transmission in Hot Fluid Injection," *Pet. Eng.* (Nov. 1964) 110.
9. Spillette, A. G.: "Heat Transfer During Hot Fluid Injection Into an Oil Reservoir," *J. Cdn. Pet. Tech.* (Oct.-Dec. 1965) 213.
10. Baker, P. E.: "Heat Wave Propagation and Losses in Thermal Oil Recovery Process," *Proc.*, Seventh World Pet. Cong., Mexico City (1968).
11. Baker, P. E.: "An Experimental Study of Heat Flow in Steamflooding," *Soc. Pet. Eng. J.* (March 1969) 89-99; *Trans.*, AIME Vol. 246.

12. Baker, P. E.: "Effect of Pressure and Rate on Steam Zone Development in Steamflooding," *Soc. Pet. Eng. J.* (Oct. 1973) 274-284; *Trans.*, AIME, Vol. 255.

13. Ersoy, D.: "Temperature Distribution and Heating Efficiency of Oil Recovery by Hot Water Injection," PhD thesis, Stanford U., Stanford, Calif. (Aug. 1969).

14. Crichlow, H. B.: "Heat Transfer in Hot Fluid Injection in Porous Media," PhD thesis, Stanford U., Stanford, Calif. (May 1972).

15. Miller, F. G.: "Steady Flow of Two-Phase Single-Component Fluids Through Porous Media," *Trans.*, AIME (1951) Vol. 192, 205-216.

16. Coats, K. H., George, W. D., Chu, C., and Marcum, B. E.: "Three-Dimensional Simulation of Steamflooding," *Soc. Pet. Eng. J.* (Dec. 1974) 573-592; *Trans.*, AIME, Vol. 257.

17. Weinstein, H. G., Wheeler, J. A., and Woods, E. G.: "Numerical Model for Steam Stimulation," paper SPE 4759 presented at the SPE-AIME Third Improved Oil Recovery Symposium, Tulsa, Okla., April 22-24, 1974.

18. Cady, G. V., Bilhartz, H. L., Jr., and Ramey, H. J., Jr.: "Model Studies of Geothermal Steam Production," *Water-1972*, AIChE Symposium Series (1972) 445-452.

19. Arihara, N.: "A Study of Non-Isothermal Single- and Two-Phase Flow Through Consolidated Sandstones," PhD thesis, Stanford U., Stanford, Calif. (Nov. 1974).

20. Klinkenberg, L. J.: "The Permeability of Porous Media to Liquids and Gases," *Drill. and Prod. Prac.*, API (1941) 200.

21. Weinbrandt, R. M., Ramey, H. J., Jr., and Cassé, F.: "The Effect of Temperature on Relative and Absolute Permeability of Sandstones," *Soc. Pet. Eng. J.* (Oct. 1975) 376-384.

22. Cassé, F. J.: "The Effect of Temperature and Confining Pressure on Fluid Flow Properties of Consolidated Rocks," PhD thesis, Stanford U., Stanford, Calif. (Nov. 1974).

23. Luikov, A. V.: *Heat and Mass Transfer in Capillary-Porous Bodies*, Pergamon Press, Inc., Elmsford, N. Y. (1966).

***